1 PERKIN

Syntheses and characterization of 5-substituted hydantoins and thiazolines—implications for crystal engineering of hydrogen bonded assemblies. Crystal structures† of 5-(2-pyridylmethylene)-hydantoin, 5-(2-pyridylmethylene)-2-thiohydantoin, 5-(2-pyridylmethylene)thiazolidine-2,4-dione, 5-(2-pyridylmethylene)rhodanine and 5-(2-pyridylmethylene)pseudothiohydantoin‡

Mubarik M. Chowdhry,§ D. Michael P. Mingos,¶ Andrew J. P. White and David J. Williams

Department of Chemistry, Imperial College of Science, Technology and Medicine, South Kensington, London, UK SW7 2AY

Received (in Cambridge, UK) 31st May 2000, Accepted 10th August 2000
First published as an Advance Article on the web 3rd October 2000

A series of six potentially bidentate ligands composed of 5-membered heterocyclic rings with methylenepyridyl substituents are described. These molecules are potentially bifunctional, acting as bidentate ligands to metal centres whilst retaining on their periphery a range of groups capable of forming triple hydrogen bonds. Their metal complexes have the potential to display interesting magnetic, optical and electrochemical properties when the hydrogen bonds are used for the crystal engineering of solid state materials. Here we report the synthesis and characterization of the six closely related molecules, 5-(2-pyridylmethylene)hydantoin **I**, 5-(2-pyridylmethylene)-2-thiohydantoin **II**, 5-(2-pyridylmethylene)thiazolidine-2,4-dione **III**, 5-(2-pyridylmethylene)rhodanine **IV**, 5-(2-pyridylmethylene)pseudothiohydantoin **V** and 5-(2-pyridylmethylene)-2-imino-4-amino-2,5-dihydrothiazole **VI**. The solid state structures of **I**–**VI** have been studied using natural abundance solid state ^{15}N NMR spectroscopy and the single crystal structures of **I**–**V** are discussed.

Introduction

The manipulation of non-covalent molecular interactions to control molecular assembly is a corner-stone in the field of supramolecular chemistry.[1] The use of triple hydrogen bonding interactions as a design principle to assemble molecular organic solids has been widely used as a particularly interesting and effective way of constructing specific supramolecular assemblies.[2–50] An extension of this principle has been to incorporate transition metal ions as part of the hydrogen bonded molecular assemblies which could potentially introduce interesting optical, electrochemical and magnetic properties into these materials and this has been recently reviewed.[51]

We have been studying the intermolecular hydrogen bonding capabilities of bifunctional molecules in transition metal complexes.[32–40,51–54] Theoretical calculations have shown that in a transition metal complex, the metal ion can influence the hydrogen bonding capability of the ligand.[55] It has also been shown that for organic molecules, the sum of the overall binding energy of complementary triply hydrogen bonding units depends on the sequence of hydrogen bond donors (**D**) or acceptors (**A**) in the molecule. Experimental[56] and theoretical[55,57] results show that the relative binding energies of the hydrogen bonding systems are **DDD/AAA** > **DDA/AAD** > **DAD/ADA**.

In this paper, the syntheses and characterisations of six closely related molecules are described (Fig. 1) as a first step to our wider synthetic strategy aimed at providing a library of bifunctional molecules capable of forming complexes with transition metals whilst retaining their ability to form triple hydrogen bonded systems with complementary units *via* molecular recognition. Molecules **I**–**IV** all have an **ADA** hydrogen bonding arrangement but incorporate subtle design differences either in the hydrogen bonding acceptor atoms (**II** and **IV**) or in their ability to act as anionic ligands (**I** and **III**) when part of a transition metal complex. Compounds **V** and **VI** are expected to form **AAD** and **DAD** hydrogen bonding arrangements respectively.[58] All the molecules contain biologically active five membered ring components. For example the 2-thiohydantoin‡ component of **II** has been used in medicinal chemistry as a component of anticonvulsant agents.[59–62] Industrially, they have been employed in textile printing,[63,64] as catalysts for polymerisation,[65] in the production of plastics and resins[66,67] and in photographic compositions.[68] Thiazolidine-2,4-dione (frequently called 'Senfölessigsäure' in the early German literature) and rhodanine derivatives have been used in qualitative and quantitative analyses of heavy metal ions and as antimicrobial, insecticidal and parasiticidal agents.[69]

We have reported previously a high yield synthetic route to stereoisomerically pure **I** as well as its crystal structure and the structures of its Ni(II) and Cu(II) metal complexes.[52] Recently we reported the crystal structure of **V** and its preferred tautomer in solution and solid states using natural abundance 2D ^{1}H–^{15}N inverse correlation NMR and ^{15}N NMR dipolar phasing experiments respectively.[58] Here we report crystal structures for **I**–**V** and present a discussion of the structural features of the PYHY series **I**–**VI**.

† CCDC reference number 207/468. Hard copy of the crystallographic data for **I** is available from CCDC. See http://www.rsc.org/suppdata/p1/b0/b004312p for crystallographic files of **II**–**V** in .cif format.

‡ IUPAC name for hydantoin is imidazolidine-2,4-dione, for rhodanine is 2-thioxothiazolidin-4-one and for pseudothiohydantoin is 2-thioxo-imidazolidin-4-one.

§ *Present address*: Laboratoire de Chimie Supramoléculaire, Institut Le Bel, Université Louis Pasteur, 4 Rue Blaise Pascal, 67000 Strasbourg, France.

¶ *Present address*: St. Edmund's Hall, Queen's Lane, Oxford, UK OX1 4AR.

DOI: 10.1039/b004312p

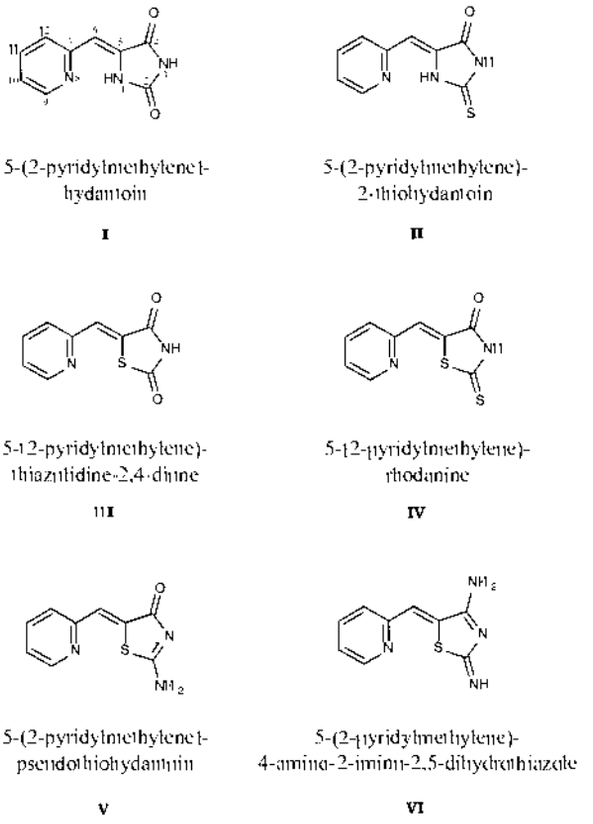

Fig. 1 Line drawings of the 'PYHY' series **I**–**VI**.

Results and discussion

Ligand syntheses

The stereoisomerically pure *Z* form of **I** was synthesised using a high yield method (70% compared with 8% for a similar method[70]). This synthetic pathway is summarised in Scheme 1. Compound **I** is soluble in chloroform, methanol, acetonitrile,

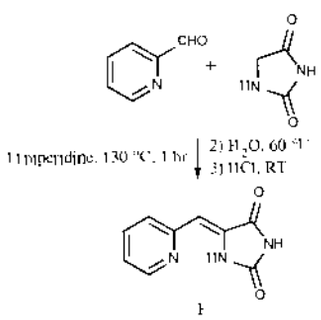

Scheme 1 Synthetic route to *Z*-isomer of **I**.

acetic acid, DMF and DMSO. The determination of its isomeric configuration was established from spectroscopic and analytical data. Recrystallisation from ethanol resulted in yellow monoclinic crystals which were found to be suitable for a single crystal X-ray diffraction study.

Attempts to synthesise molecules **II**–**VI** using the method described for **I** yielded a mixture of insoluble products. An alternative synthetic route shown in Scheme 2 proved to be more efficient.

The syntheses of **II**–**IV** were carried out in a one pot reaction where the five membered heterocyclic ring component was reacted in a 1:1 ratio with the aldehyde in the presence of glycine, sodium carbonate and water and the mixture was stirred at 25 °C (110 °C for **III** and **IV**) for 1 h (2 h for **IV**). The resulting precipitate was isolated and gave micro-analytical data supporting the formulation of the desired compound.

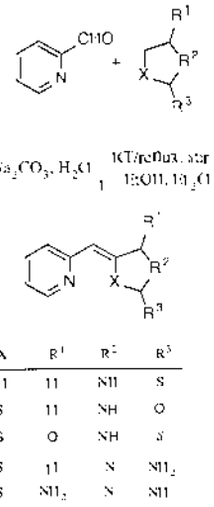

	X	R^1	R^2	R^3
II	NH	H	NH	S
III	S	H	NH	O
IV	S	O	NH	S
V	S	H	N	NH_2
VI	S	NH_2	N	NH

Scheme 2 Synthetic strategy for the syntheses of **II**–**VI**.

The yields of the molecules are a great improvement over those previously reported for **I**, **II** and **IV**. The observed melting point for **II** agreed well with that reported by Thielemann[70] but was lower than that quoted by Montaña González and coworkers.[71] The high yields obtained using this route may be due to the amphoteric nature of glycine in water, thereby promoting the condensation reaction much more effectively than using sequential acid and base reagents. The formation of the *E*-isomer is not favourable due to electrostatic repulsions experienced by the R^1 group at the 4-position and the pyridyl nitrogen atom at the 8-position as shown in Scheme 2. Conversely the formation of the *Z*-isomer where X = NH is known to be favoured by the formation of an intramolecular hydrogen bond as described for **I**[72] and therefore the *Z*-isomer is expected for **II**. For **III**–**VI** where X = S this conformation may also be favoured due to electrostatic attractions of the lone pair of pyridyl nitrogen and the ring sulfur atom.

^{1}H NMR spectroscopy

The ^{1}H NMR data for **I**–**VI** are summarized in Table 1 and those for **I**, **II** and **IV** are in agreement with those reported in the literature (see structure **I** in Fig. 1 for the numbering system used).[72,73] The *Z*- and *E*-isomers of **I**–**VI** have characteristic chemical shifts for the H(6) proton. However, the presence of only one signal for H(6) suggests the exclusive formation of only one stereoisomer. For **I**–**IV**, the broad and overlapping downfield signals between 10–14 ppm are assigned to H(1) and/or H(3) and suggest proton exchange between the two nitrogens of the five membered ring on the NMR timescale. Compound **V** shows the presence of the aromatic protons H(9)–H(12) at a chemical shift range of 7.34 to 8.69 ppm and the methylene proton, H(6) at 7.63 ppm. Two singlets at 9.09 and 9.32 ppm are assigned to the NH protons, which suggest that in solution, **V** exists either as the amino tautomer with hindered rotation about the C(2)–N(2) bond or as the imino tautomer. Two-dimensional ^{1}H–^{15}N solution state NMR studies in d_6-DMSO have shown that the amino tautomeric form of **V** is preferred.[58] Due to the interactive and eventual destructive effects of d_6-DMSO on **VI**, deuterated DMF and acetic acid were also used. Spectra recorded in d_6-DMSO and d_7-DMF gave resonances attributable to the N–H protons, but which were too broad to assign individually.

^{13}C NMR spectroscopy

^{13}C{H} NMR spectroscopic data for **I**–**VI** were recorded in both solid and solution states and data for C(2) and C(6) are summarized in Table 2. The C–H coupling constants for the solution state are only given for **I** as those observed for **II**–**VI** were found to be very similar.[74]

Table 1 ^{1}H NMR data for **I**–**VI** in d_6-DMSO solution (δ in ppm)

Comp.	δH(1)	δH(3)	δH(6)	δH(9)	δH(10)	δH(11)	δH(12)
I	10.34	11.32	6.49	8.64	7.80	7.27	7.57
II	12.32	11.55	6.62	8.74	7.88	7.37	7.73
III	—	12.46	7.84	8.76	7.88	7.43	7.87
IV	—	13.70	7.70	8.80	7.97	7.45	7.94
V	9.32[a]	9.09[a]	7.63	8.69	7.86	7.34	7.74
VI	—	—	7.80	8.75	7.91	7.38	7.54

[a] Amino protons.

Table 2 ^{13}C NMR data for C(2) and C(6) of molecules **I**–**VI** (δ in ppm, J in Hz, values in parentheses are for the solid state)

Comp.	δC(2)	δC(6)
I	154.68 (151.34)	104.98 (107.46) $^1J_{C-H}$ = 163.0, $^2J_{C-H}$ = 3.1
II	179.37 (177.9)	107.88 (108.5)
III	172.72 (178.5)	128.67 (132.6)
IV	202.66 (203.2)	124.66 (123.6)
V	180.81 (180.8)	125.83 (127.9)
VI	175.88 (180.8)	122.63 (120.0)

Table 3 Natural abundance high resolution solid state ^{15}N NMR data (δ in ppm) for the ligands **I**–**VI** and ^{13}C solid state NMR data for C(2) for comparison

Comp.	δN(1)	δN(2)	δN(3)	δN(8)	δC(2)
I	−264	n/a	−236	−83	151.3
II	−236	n/a	−214	−73	177.9
III	n/a	n/a	−217	−74	178.5
IV	n/a	n/a	−192	−70	203.2
V	n/a	−266	−160	−68	180.8
VI	n/a	−285	−156	−68	180.8

In general, the variation in chemical shift between the solid and solution states of the ligands is small. For ease of comparison between the ligands, the ^{13}C chemical shifts of the ligands **II**–**VI** in the solid state are arbitrarily referenced to those of **I**. It is clear that the most significant change in chemical shift between molecules **I**–**VI** occurs for the C(2) atom. In **II**, the introduction of a ring sulfur atom α to C(2) results in a downfield chemical shift of *ca.* 28 ppm relative to **I**. A slightly larger shift of *ca*. 27 ppm is observed for **III** where the sulfur atom resides in an exocyclic position in the thiocarbonyl group. A deviation of *ca.* 52 ppm was recorded for **IV**; which correlates well with a calculated value of 53 ppm from the sum of the individual chemical shift deviations for C(2) observed for **II** and **III**, and can be rationalised on the basis of there being both a ring and an exocyclic sulfur atom α to C(2). A difference of *ca*. 25 ppm is observed for C(6) on comparison of **I** and **III** which contain an NH group and sulfur atom at position 1 respectively.

Natural abundance high resolution solid state ^{15}N NMR spectroscopy

The ^{15}N NMR spectroscopic data obtained for **I**–**VI** are summarised in Table 3. The N(8) and N(3) chemical shifts for **I** and **III** are lower than those observed for **II** and **IV**, respectively. The substitution of a thiocarbonyl for a carbonyl group results in an upfield shift for all the nitrogen signals. This effect is particularly noticeable when compared with the signals for N(1) from **I** and **II**. Strikingly similar changes of 22 and 25 ppm for the signal for N(3) are also observed on comparison of **I** and **II** with **III** and **IV**. The trends observed in the chemical shifts for N(3) are analogous to the trends observed for the variation in the chemical shift of C(2) in the ^{13}C NMR spectra for **I**–**VI**. We have previously given a detailed discussion on the ^{15}N NMR spectra in the solution and solid states of **V** in order to identify its preferred tautomeric form.[58] A poorly resolved spectrum for **VI** gave three signals: a relatively sharp signal at −68 ppm, a broad signal at −156 ppm and a considerably broader signal at *ca*. −285 ppm which were assigned to N(8), N(3) and N(2) respectively. The lack of a discrete signal for N(4) could be due to two reasons. Firstly, it is reported that thiazolines can undergo substitution of the N(4)H_2 group for a carbonyl in the presence of water.[75] Secondly, the signal may be hidden in the poorly resolved and broad nature of the signals assigned to N(3) and N(2) in the spectrum. In order to investigate the former, an accurate FAB$^+$ mass spectrum of **VI** was recorded (*vide infra*).

Infra-red spectroscopy

The subtle differences in molecular structures associated with the ligands **I**–**VI** are reflected in their IR spectral characteristics. Table 4 compares the assignments of the IR bands observed for these ligands recorded as KBr pellets. The ν(N–H) stretching modes show two strong broad bands at *ca*. 3100–3170 and 3050 cm^{-1} for the N(3)–H stretching mode for **I**–**IV**. The N(2)–H stretching modes for **V** are observed at 3196, 2967 and 2878 cm^{-1}. For **I** and **II**, an additional sharp band at *ca*. 3270 cm^{-1} is observed and is assigned to the N(1)–H stretching mode; the lower frequency and increased sharpness of this band is probably due to the formation of an intramolecular hydrogen bond between N(1)–H and N(8). The carbonyl stretching frequencies are in the range 1670–1775 cm^{-1}. The specific assignments have been inferred from the extent of involvement of the carbonyl oxygen atom in intermolecular hydrogen bond formation (which has been determined from X-ray structural analysis (*vide infra*)). A comparison of the ν(C=C) stretching mode in the ligands **I**–**VI** generally reveals a shift to lower wavenumbers from 1669 cm^{-1} in **I** to 1604 cm^{-1} in **VI**. It is interesting to note that the introduction of an *exocyclic* sulfur atom in **II** and **IV** also leads to a decrease in wavenumbers for the ν(C=C) stretching mode of 9 and 11 cm^{-1} from **I** to **II** and **III** to **IV**, respectively. These shifts increase if a *ring* sulfur atom is introduced; the ν(C=C) stretching mode being shifted −53 and −55 cm^{-1} from **I** to **III** and **II** to **IV**, respectively. Conversely, a progressive increase in wavenumbers for the asymmetric (C–N–C) stretching mode is observed from **I** through to **IV**. The spectral bands of **VI** are markedly broader than those obtained for **I**–**V**. A very strong broad band from 3600–2600 cm^{-1} is assigned to ν(N–H) hydrogen bonded stretching modes. Between 1600–1250 cm^{-1}, there are strong, broad, overlapping bands due to δ(N–H) deformation of the thiazoline ring and ν(C=N) stretching modes of the pyridyl ring.

Accurate FAB$^+$ mass spectrometry

The determination of the presence of an amino or carbonyl group at the 4-position of **VI** (denoted **VI**^{a} and **VI**^{c} respectively) could not be determined by IR spectroscopy due to the presence of strong overlapping broad bands in the N–H and C=O stretching and bending regions. The lower solubility and stability of **VI** compared with **I**–**V** in common solvents have limited progress to obtain crystals suitable for an X-ray diffraction

Table 4 Selected infra-red spectroscopic band assignments (cm^{-1}) for **I**–**VI**

Comp.	ν(N–H)	ν(C=O)	ν(C=C)	ν(C=S)	ν(ring, py)	$\nu(C–S)_{ring}$	δ(N–H)	ν_{as}(C–N–C)	δ(C=S)	$\delta(C–H)_{ip}$	$\delta(C–H)_{oop}$
I	3270	1775 (O4)	1669	—	1587	—	1367	1153	—	788	563
	3166	1716 (O2)			1463						553
II	3059										
	3275	1720	1660	1261	1584	—	1358	1161	889	781	556
	3153			1110	1469				682		
III	3059										
	3134	1741 (O2)	1616	—	1582	910	1340	1168	—	780	532
	3044	1681 (O4)			1472		1445				
IV	3096	1725	1605	1148	1580	917		1187	878	781	523
	3047			1082	1472				684		
V	3196										
	2967	1670	1617	—	1582	895	1495	1146	—	780	553
	2878				1471		1375				551
VI	3600–2600						1511				
		—	1604	—	1583	896	1434	1151	—	777	528
					1469	867	1351				

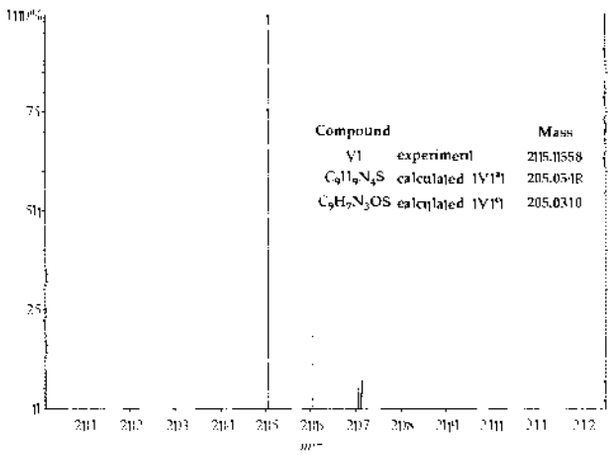

Fig. 2 Accurate FAB^+ mass spectrum obtained for **VI**. The inset table compares the experimentally observed mass with calculated values for $[\mathbf{VI}]^+$ with either an amino substituent ($\mathbf{VI}^a$) or a carbonyl ($\mathbf{VI}^c$) at the 4-position (experimental error limits are ±10 mDa).

study. Data from an accurate mass FAB^+ spectroscopic analysis of **VI** shown in Fig. 2, suggested the correct empirical formula of the product to be $\mathbf{VI}^a$.

This suggests that in the ^{15}N NMR spectrum for **VI**, the chemical shift signal of the N(4) atom is probably part of one of the broad bands observed in the spectrum and its position is tentatively predicted to be superimposed on the N(2) amino signal at −285 ppm.

Molecular and crystal structures

The X-ray structures of compounds **I**–**V** have been determined and show each of the molecules to have a *Z* configuration about the C(5)–C(6) bond. Selected bond lengths, angles and derived parameters for each of the structures are shown in Table 5, and the structures of two representative examples of the five molecules are shown in Fig. 3 (compound **II**) and Fig. 4 (compound **V**). All five structures are essentially planar, with the mean deviations from planarity ranging between 0.02 Å in **I** to 0.13 Å in **II**. The out-of-plane deviations are principally a consequence of small torsional twists about the C(6)–C(7) bond which range from 0.7(4)° in **IV** to 12.1(3)° in **II**. In all five structures there is a marked pattern of bond delocalisation in the five-membered heterocyclic rings [with the exception of the C(4)–C(5) bond], a pattern that extends to include the C(5)–C(6) and C(6)–C(7) bonds (and the attached pyridyl ring), the C(5)–C(6) double bond showing a loss of double bond character. The most noticeable variation in this pattern of bonding is in **V** where the presence of the amino substituent is accompanied by a significant shortening of the C(2)–N(3) bond length *cf*. its value in the other four structures.

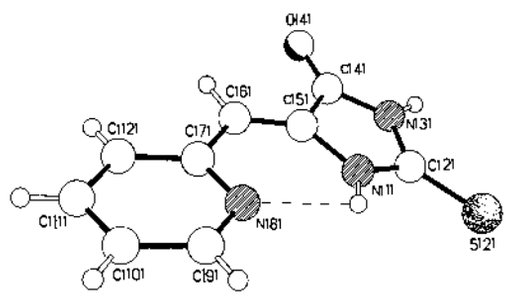

Fig. 3 Molecular structure of **II** showing the intramolecular N–H · · · N hydrogen bond.

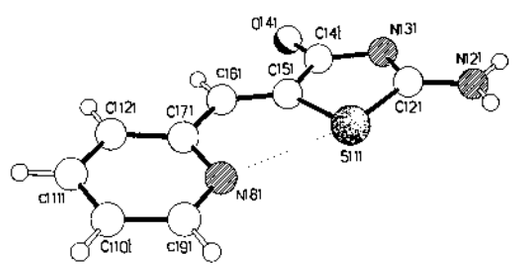

Fig. 4 Molecular structure of **V** showing the intramolecular S · · · N contact.

The near co-planarity of the two ring systems is consistent with the pronounced conjugative interaction present in all five molecules. In **I** and **II**, this geometry favours, or is reinforced by, the presence of an intramolecular hydrogen bond between N(1) and N(8). This hydrogen bond is noticeably longer in **II** than in **I**, probably due to the differing influence of intermolecular hydrogen bonds involving the thiohydantoin/hydantoin ring systems respectively (*vide infra*). The longer hydrogen bond in **II** is accompanied by an enlargement of the internal angle at C(6). Although in **III**, **IV** and **V**, there is no intramolecular hydrogen bond constraining the geometry, a co-planar conformation for the two rings in these compounds is still favoured by the formation of a 'proto' bond between S(1) and N(8). The precedent for this type of interaction is well established [76–88] and indeed in some instances a formal bond has been proposed,[76] though in this latter example there is a second sulfur atom α to the S(1) sulfur centre. The presence of carbonyl, thiocarbonyl or amino groups in the α position for **III**, **IV** and **V** respectively clearly weakens this S · · · N interaction, the internal angle at C(6) in all cases being significantly enlarged from trigonal *cf.* that observed in related systems.[76–88] However, this is to be expected since the replacement of sulfur by carbonyl, thiocarbonyl or

Table 5 Selected bond lengths (Å), angles (°) and derived parameters for **I**–**V**

	I X = N, Y = O	**II** X = N, Y = S	**III** X = S, Y = O	**IV** X = S, Y = S	**V** X = S, Y = N
X(1)–C(2)	1.362(2)	1.359(3)	1.769(2)	1.751(3)	1.768(2)
X(1)–C(5)	1.388(2)	1.384(3)	1.751(2)	1.752(2)	1.741(2)
C(2)–Y(2)	1.206(2)	1.633(2)	1.215(2)	1.639(3)	1.307(2)
C(2)–N(3)	1.401(2)	1.379(3)	1.369(2)	1.363(3)	1.329(2)
N(3)–C(4)	1.361(3)	1.366(3)	1.376(2)	1.379(3)	1.357(2)
C(4)–O(4)	1.216(2)	1.217(2)	1.209(2)	1.214(3)	1.223(2)
C(4)–C(5)	1.480(3)	1.481(3)	1.489(2)	1.482(3)	1.495(2)
C(5)–C(6)	1.336(3)	1.340(3)	1.338(2)	1.334(4)	1.338(3)
C(6)–C(7)	1.461(3)	1.452(3)	1.457(2)	1.455(4)	1.459(3)
C(7)–N(8)	1.347(2)	1.348(3)	1.346(2)	1.344(4)	1.340(3)
N(8)–C(9)	1.338(3)	1.332(3)	1.329(2)	1.335(3)	1.335(3)
X(1)···N(8)	2.743(2)	2.899(3)	2.813(1)	2.808(2)	2.805(2)
H···N(8)	2.06	2.41	—	—	—
X(1)–H···N(8)	132	115	—	—	—
C(2)–X(1)–C(5)	112.0(2)	111.6(2)	90.9(1)	92.3(1)	88.0(1)
X(1)–C(2)–Y(2)	128.3(2)	128.6(2)	123.5(1)	123.3(2)	119.8(1)
X(1)–C(2)–N(3)	105.6(2)	106.2(2)	111.3(1)	110.3(2)	117.5(1)
Y(2)–C(2)–N(3)	126.1(2)	125.1(2)	125.2(1)	126.5(2)	122.7(2)
C(2)–N(3)–C(4)	112.0(2)	112.2(2)	117.1(1)	117.9(2)	111.1(2)
N(3)–C(4)–O(4)	126.7(2)	127.1(2)	124.0(1)	123.0(2)	124.2(2)
N(3)–C(4)–C(5)	105.2(2)	104.8(2)	109.8(1)	109.8(2)	113.6(2)
O(4)–C(4)–C(5)	128.1(2)	128.1(2)	126.2(1)	127.2(2)	122.2(2)
X(1)–C(5)–C(4)	105.2(1)	105.1(2)	110.9(1)	109.7(2)	109.6(1)
X(1)–C(5)–C(6)	128.3(3)	131.1(2)	127.7(1)	128.4(2)	127.7(1)
C(4)–C(5)–C(6)	126.5(2)	123.6(2)	121.4(1)	121.9(2)	122.7(2)
C(5)–C(6)–C(7)	125.6(2)	127.3(2)	125.6(1)	125.5(2)	125.2(2)
C(6)–C(7)–N(8)	116.7(2)	117.3(2)	116.6(1)	116.0(2)	116.4(2)
A[a]	0.7(3)	−2.6(3)	−1.4(3)	1.9(4)	1.5(3)
B[b]	0.8(3)	12.1(3)	3.5(2)	0.7(4)	8.6(3)
C[c]	0.019	0.132	0.049	0.033	0.105
D[d]	0.049 [N(8)]	0.280 [C(11)]	0.094 [N(8)]	0.092 [O(4)]	0.215 [C(9)]

[a] *A* is the mean torsional twist (°) about the C(5)–C(6) bond. [b] *B* is the mean torsional twist (°) about the C(6)–C(7) bond. [c] *C* is the mean deviation from planarity (Å) of the molecule. [d] *D* is the maximum deviation from planarity (Å) of the molecule.

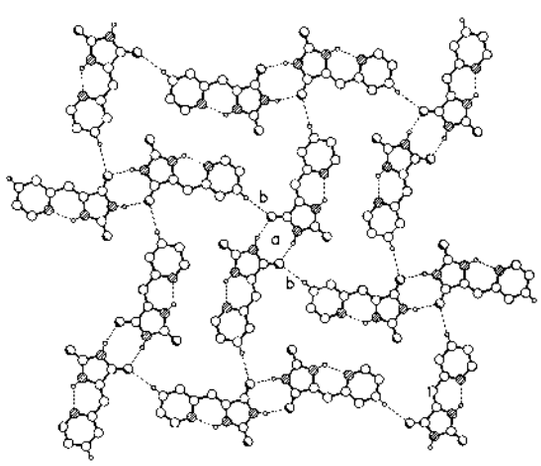

Fig. 5 Part of one of the parquet-like hydrogen bonded sheets present in the structure of **I**. Hydrogen bonding geometries: [X···Y, H···Y in Å and X–H···Y in °] **a**, 2.86, 1.98, 164; **b**, 3.39, 2.44, 170 (N–H 0.90 Å, C–H 0.96 Å).

amino represents a change from an electron donating atom, which favours the formation of a strong S(1)···N(8) 'bond', to an electron withdrawing group which weakens this interaction and hence causes the observed increase in the S(1)···N(8) separation.

Inspection of the packing of the molecules reveals a feature common to all five structures, *i.e.* the formation of C_i related hydrogen bonded dimer pairs (this hydrogen bond is identified as **a** in each of Figs. 5 and 7–10). In each case this hydrogen bonding is between the N(3) ring nitrogen atom of one molecule and either the O(4) or the X(2) substituent of the other. In

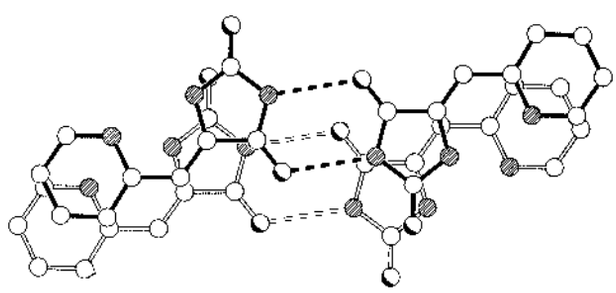

Fig. 6 An illustration of the π–π overlap present between parallel stacked dimer pairs in the crystals of **I**.

I, **II** and **III** these hydrogen bonds are N(3)–H···O type interactions, whereas in **IV** the hydrogen bond is from N(3)–H to the sulfur atom S(2) rather, than as anticipated, to the carbonyl oxygen atom O(4). In **V**, N(3) acts as an acceptor of a hydrogen bond from one of the amino N–H hydrogen atoms. In **I**–**IV** these dominant hydrogen bonding patterns are supplemented by weaker, secondary interactions. This leads in **I** to the formation of a parquet-like sheet structure *via* a C–H···O hydrogen bond (**b** in Fig. 5) between the hydrogen *para* to the pyridine nitrogen atom in one molecule and the carbonyl oxygen atom O(4) of another (the oxygen atom also utilised in the dimer pair formation). Adjacent sheets are stacked parallel to each other with near optimal overlap of the pyridyl rings (Fig. 6) consistent with π–π stacking (mean interplanar separation 3.42 Å, centroid···centroid distance 3.81 Å). In **II** the secondary interaction is between the N(1)–H hydrogen atom of one molecule and the sulfur atom S(2) of another (identified as **b** in Fig. 7) resulting in the formation of 'tapes'. Lattice translated tapes are layered with each other (mean interplanar separation

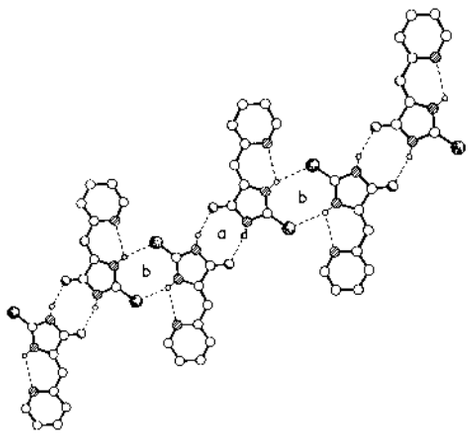

Fig. 7 Part of one of the hydrogen bonded tapes present in the structure of **II**. Hydrogen bonding geometries: [X · · · Y, H · · · Y in Å and X–H · · · Y in °] **a**, 2.85, 1.99, 161; **b**, 3.56, 2.71, 158 (N–H 0.90 Å).

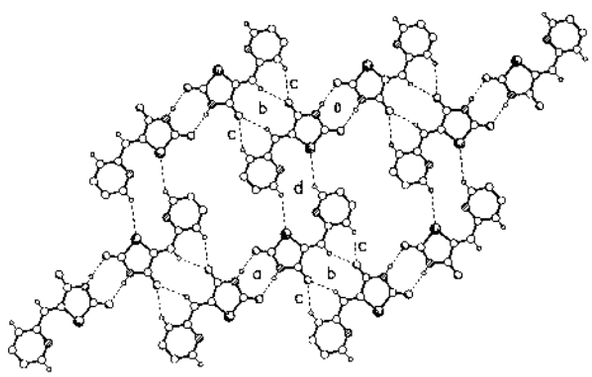

Fig. 8 Part of one of the weakly cross-linked hydrogen bonded sheets present in the structure of **III**. Hydrogen bonding geometries: [X · · · Y, H · · · Y in Å and X–H · · · Y in °] **a**, 2.85, 1.95, 175; **b**, 3.32, 2.51, 142; **c**, 3.40, 2.61, 140; **d**, 3.74, 2.92, 144 (N–H 0.90 Å, C–H 0.96 Å).

ca. 3.5 Å), the pyridyl rings within one tape partially overlaying the thiohydantoin rings of another. Symmetry related tapes are inclined to each other by *ca*. 40° and intermesh with each other, there being no significant inter-tape interactions other than normal van der Waals. In **III** there are close approaches (labelled as **b** and **c** in Fig. 8) between the C(6)–H and C(12)–H hydrogen atoms respectively of one molecule and the O(4) carbonyl oxygen atom of another (that not involved in dimer pair formation) producing weakly linked tapes. The C(9)–H pyridyl hydrogen atoms of one tape are in a proximal relationship with the sulfur atoms of another, and *vice versa* (contact **d** in Fig. 8) resulting in the formation of a near planar sheet-like array. Adjacent sheets are aligned parallel to each other with the C(5)–C(6) double bonds in one sheet lying over the pyridyl rings of the next at a distance of *ca*. 3.5 Å. A similar pattern of inter-dimer interactions (denoted as **c**, **d** and **b** respectively in Fig. 9) is also present in the structure of **IV**, leading again to sheets that stack (mean interplanar separation *ca*. 3.5 Å). Here the pyridyl and rhodanine rings within one sheet overlay their counterparts in the next, an overlap pattern directly analogous to that observed in **I** (illustrated in Fig. 6). In **V**, hydrogen bonded dimers are linked *via* pairs of strong N–H · · · O hydrogen bonds between the amino N(2)–H hydrogen atom not involved in dimer formation in one pair and the carbonyl oxygen atom O(4) in another (**b** in Fig. 10) creating hydrogen bonded tapes. Associated with these tapes is a close approach between the carbonyl oxygen atoms in one molecule and the S(1) sulfur centres in the next (contact **c** in Fig. 10). The tapes stack parallel to each other with the amino nitrogen atoms within one tape lying approximately over the centre of the pyridyl rings of the next at a distance of *ca*. 3.3 Å.

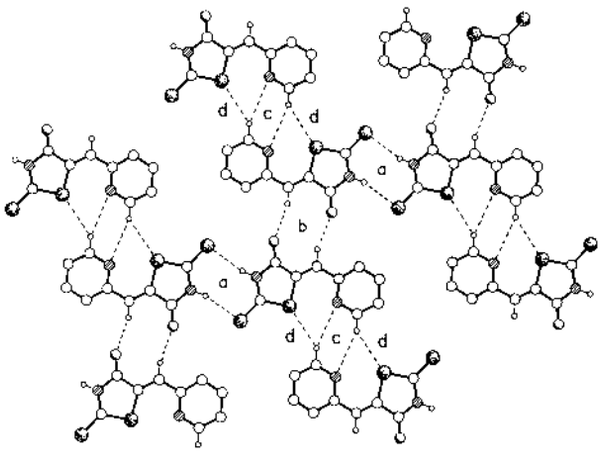

Fig. 9 Part of one of the hydrogen bonded sheets present in the structure of **IV**. Hydrogen bonding geometries: [X · · · Y, H · · · Y in Å and X–H · · · Y in °] **a**, 3.38, 2.50, 164; **b**, 3.24, 2.34, 155; **c**, 3.81, 2.91, 156; **d**, 3.72, 2.91, 143 (N–H 0.90 Å, C–H 0.96 Å).

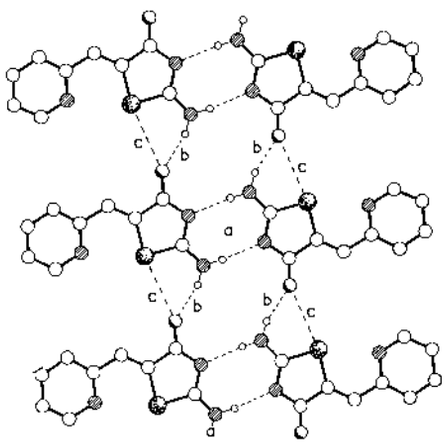

Fig. 10 Part of one of the hydrogen bonded tapes present in the structure of **V**. Hydrogen bonding geometries: [X · · · Y, H · · · Y in Å and X–H · · · Y in °] **a**, 2.93, 2.03, 174; **b**, 2.79, 1.92, 163 (N–H 0.90 Å) and non-bonded contact **c**, 3.23.

Overall, although all of these structures have supramolecular features in common, **IV** is unusual in that the dimer does not utilise the available strong N–H · · · O interaction (preferring the weaker N–H · · · S), and **II** does not form parallel stacks but is instead comprised of intermeshed sheets.

Conclusion

A series of six potentially bidentate ligands which are capable of forming triple hydrogen bonds are described. General synthetic routes to these compounds have been described and their detailed spectroscopic and structural features have been discussed. In a subsequent paper complexes of these ligands will be described.

Experimental

General

Standard synthetic techniques for handling air and moisture stable compounds were employed unless otherwise stated. Solvents were of reagent grade and used as purchased from Aldrich. Dimethyl sulfoxide was stored over barium oxide. Starting materials were purchased from Aldrich and Lancaster and used without further purification.

Infra-red spectra were recorded on Perkin-Elmer 1720 and Mattson Infra-red Fourier Transform Spectrometers between 4000 and 260 cm^{-1} as KBr pellets. ^{1}H, ^{13}C and $^{13}C\{^{1}H\}$ NMR

spectra were recorded on JEOL JNM-EX270 (^{1}H at 270 MHz and ^{13}C{^{1}H} at 67.5 MHz) and Bruker DRX-400 (^{1}H at 400 MHz and ^{13}C{^{1}H} at 100 MHz) Fourier-Transform NMR spectrometers. ^{1}H and ^{13}C NMR chemical shifts are reported in parts per million (δ) relative to TMS ($\delta = 0$) using $(CD_3)_2SO$ ($\delta_H = 2.52$) unless stated. ^{13}C NMR data are referenced to $(CD_3)_2SO$ ($\delta_C = 43.5$). Coupling constants are reported in Hz. The solid state ^{13}C NMR spectra were recorded on a Bruker MSL300 spectrometer (^{13}C{^{1}H} at 75.5 MHz) and the solid state ^{15}N spectra were recorded on the same spectrometer at 30.4 MHz using magic-angle spinning (MAS). Chemical shifts are given relative to external liquid nitromethane using solid $^{15}NH_4NO_3$ as a secondary reference. Positive ion FAB and chemical ionisation mass spectra were recorded on a VG AutoSpec-Q using 3-nitrobenzyl alcohol as matrix for the former and ammonia for the latter.

Synthesis of 5-(2-pyridylmethylene)imidazolidine-2,4-dione I

A one necked 250 cm^3 round bottom flask was charged with pyridine-2-carbaldehyde (5.36 g, 50 mmol), hydantoin (5.50 g, 55 mmol) and piperidine (10 cm^3). The orange mixture was slowly heated to 130 °C with stirring and maintained at this temperature for 1 h. The mixture was then cooled to 60 °C and water (200 cm^3) was added. Stirring was continued until the mixture reached room temperature and all solid material had dissolved (approx. 1 h). The product was precipitated by addition of concentrated hydrochloric acid (7 cm^3), filtered, washed with cold water (5 cm^3) and ethanol (5 cm^3) and was found to be pure by TLC. For elemental analysis, the product was recrystallised from a hot ethanolic solution. Single crystals were grown from slow cooling (over 24 h) of a hot ethanolic solution containing the ligand and then allowing slow evaporation of the solvent over two days. HPYHY, **I**, is soluble in MeOH, MeCN, DMF and DMSO. Yield: 6.65 g, 70%, mp 222 °C (lit. 220–223 °C[89]). Found: C, 57.2; H, 3.6; N, 22.0%. Calc. for $C_9H_7N_3O_2$: C, 57.1; H, 3.7; N, 22.2%. ^{1}H NMR (d_6-DMSO): δ 6.49 (H[6], s, 1H), 7.27 (H[11], ddd, $^3J(^1H,^1H)$ 7.6, $^4J(^1H,^1H)$ 4.8, $^5J(^1H,^1H)$ 1.0 Hz, 1H), 7.57 (H[12], d, $^3J(^1H,^1H)$ 7.9 Hz, 1H), 7.80 (H[10], dt, $^3J(^1H,^1H)$ 7.7, $^4J(^1H,^1H)$ 1.8 Hz, 1H), 8.64 (H[9], dd, $^3J(^1H,^1H)$ 4.8, $^4J(^1H,^1H)$ 1.0 Hz, 1H), 10.34 (H[1], s, 1H), 11.32 (H[3], s, 1H). ^{13}C NMR (d_6-DMSO): δ 165.14 (C[4]), 154.68 (C[2]), 153.70 (C[7]), 149.42 (C[9], $^1J(^{13}C,^1H)$ 181, $^2J(^{13}C,^1H)$ 9.2, $^3J(^{13}C,^1H)$ 3.6 Hz), 137.09 (C[11],$^1J(^{13}C,^1H)$ 165, $^2J(^{13}C,^1H)$ 6.1 Hz), 131.77 (C[5], $^2J(^{13}C,^1H)$ 4.9 Hz), 125.45 (C[12], $^1J(^{13}C,^1H)$ 165, $^2J(^{13}C,^1H)$ 6.7 Hz), 122.29 (C[10], $^1J(^{13}C,^1H)$ 166 $^2J(^{13}C,^1H)$ 7.3 Hz), 104.98 (C[6],$^1J(^{13}C,^1H)$ 163, $^2J(^{13}C,^1H)$ 3.1 Hz). ^{13}C (high resolution solid-state) NMR: δ 167.92 (C[4]), 151.34 (C[2], C[7]), 148.98 (C[9]), 137.12 (C[11]), 130.69 (C[5]), 128.12 (C[12]), 123.54 (C[10]), 107.46 (C[6]). ^{15}N{^{1}H} MAS-CP NMR solid state: δ −83 (N8), −236 (N3), −264 (N1). IR (ν_{max}/cm^{-1}): 3270, (sh), ν(N–H[1]); 3166, 3059, (br), ν(N–H[3]); 2431, 2372, 2319, (br), ν(N–D); 1775, (s), ν(C(4)=O(4)); 1716, (s), ν(C(2)=O(2)); 1669, (s), ν(C=C); 1587, 1463, (s), ν(ring, py); 1367, (vs), δ(N–H); 1299, 1272, (s), δ(N–D); 1153, (s), ν(C–N–C); 788, (s), $\delta(C–H)_{ip}$; 563, 553, (s), $\delta(C–H)_{oop}$. MS CI (ammonia) {*m*/*z* [species]}: 190 $[M + H]^+$.

Synthesis of 5-(2-pyridylmethylene)-2-thioxoimidazolidin-4-one II

Pyridine-2-carbaldehyde (0.500 g, 4.66 mmol, 1 eq.) was added dropwise to a flask containing 2-thiohydantoin (0.542 g, 4.66 mmol, 1 eq.), glycine (0.350 g, 1 eq.), and sodium carbonate (0.247 g, 0.5 eq.) followed by distilled water (3 cm^3). Upon stirring, vigorous effervescing was observed and the mixture was stirred at reflux for 1 h. The bright yellow precipitate was collected and washed with water and dried *in vacuo* to give a bright yellow powder which did not require further purification. Yield: 0.860 g, 89%, mp 260–261 °C (lit. 262 °C[70]). Found: C, 52.3; H, 3.3; N, 20.2%. Calc. for $C_9H_7N_3OS$: C, 52.7; H, 3.4; N, 20.5%. ^{1}H NMR (d_6-DMSO): δ 6.62 (H[6], s, 1H), 7.37 (H[11], ddd, $^3J(^1H,^1H)$ 7.6, $^4J(^1H,^1H)$ 5.9, $^5J(^1H,^1H)$ 1.0 Hz, 1H), 7.73 (H[12], d, $^3J(^1H,^1H)$ 7.9 Hz, 1H), 7.88 (H[10], dt, $^3J(^1H,^1H)$ 7.9, $^4J(^1H,^1H)$ 1.7 Hz, 1H), 8.74 (H[9], d, $^3J(^1H,^1H)$ 4.3 Hz, 1H), 11.55 (H[1] s(br), 1H), 12.32 (H[3] s(br), 1H). ^{13}C{^{1}H} NMR (d_6-DMSO): δ 179.37 (C2), 166.29 (C4), 153.87 (C7), 150.44 (C9), 138.04 (C11), 132.08 (C5), 127.16 (C12), 123.71 (C10), 107.88 (C6). ^{13}C solid state: δ 177.9 (C2), 168.7 (C4), 152.7 (C7), 150.8 (C9), 139.2 (C11), 131.2 (C5), 128.6 (C10), 128.3 (C12), 108.5 (C6). ^{15}N{^{1}H} MAS-CP NMR solid state: δ −73 (N8), −214 (N3), −236 (N1). IR (ν_{max}/cm^{-1}): 3275, (sh), ν(N–H[1]); 3153, 3059, (m, br), ν(N–H[3]), 1720, (s), ν(C=O); 1660, (s), ν(C=C); 1584, 1469, (s), ν(N=C, py); 1358, (s), δ(N–H); 1261, 1110, (s), ν(C=S); 1161, (s), ν(C–N–C); 889, 682, (s), δ(C=S); 781, (s), $\delta(C–H)_{ip}$; 556, (s), $\delta(C–H)_{oop}$. MS FAB$^+$ (NBA) {*m*/*z* [species]}: 206 $[M + H]^+$.

Synthesis of 5-(2-pyridylmethylene)thiazolidine-2,4-dione III

Pyridine-2-carbaldehyde (1.00 g, 9.32 mmol, 1 eq.) was added dropwise to a 50 cm^3 round bottomed flask containing thiazolidine-2,4-dione (0.992 g, 9.32 mmol, 1 eq.), glycine (0.700 g, 1 eq.), and sodium carbonate (0.494 g, 0.5 eq.) followed by distilled water (2 cm^3). Upon stirring, both a bright yellow precipitate and a yellow solution resulted. A further addition of distilled water (2 cm^3) was made and the precipitate redissolved upon heating to reflux for 1 h. The solution was allowed to cool to room temperature and the yellow precipitate collected, washed with ethanol and diethyl ether and air dried to give a yellow powder which did not require further purification. Yield: 1.632 g, 85%, mp 224 °C. Found: C, 52.4; H, 2.9; N, 13.5%. Calc. for $C_9H_7N_3OS$: C, 52.4; H, 2.9; N, 13.6%. ^{1}H NMR (d_6-DMSO): δ 7.43 (H[11], ddd, $^3J(^1H,^1H)$ 7.3, $^4J(^1H,^1H)$ 4.8, $^5J(^1H,^1H)$ 1.2 Hz, 1H), 7.84 (H[6], s, 1H), 7.87 (H[12], d, $^3J(^1H,^1H)$ 7.9 Hz, 1H), 7.88 (H[10], dt, $^3J(^1H,^1H)$ 7.4, $^4J(^1H,^1H)$ 1.4 Hz, 1H), 8.76 (H[9], d, $^3J(^1H,^1H)$ 4.5 Hz, 1H), 12.46 (H[1], s(br), 1H). ^{13}C{^{1}H} NMR (d_6-DMSO): δ 172.72 (C2), 168.18 (C4), 151.97(C9), 150.03 (C7), 138.17 (C11), 128.67 (C6), 128.47 (C12, 10), 124.58 (C5). ^{13}C solid state: δ 178.5 (C2), 167.2 (C4), 152.5 (C9), 151.0 (C7), 138.6 (C11), 132.6 (C6), 128.7 (C12, C10), 124.4 (C5). ^{15}N{^{1}H} MAS-CP NMR solid state: δ −74 (N8), −217 (N3). IR (ν_{max}/cm^{-1}): 3134, 3044, (m, br), ν(N–H); 1741, (s), ν(C(2)=O(2)); 1681, (s), ν(C(4)=O(4)); 1616, (s), ν(C=C); 1582, 1472, (s), ν(N=C, py); 1340, (s), δ(N–H); 1168, (s), ν(C–N–C); 910, (s), $\nu(C–S)_{ring}$; 780, (s), $\delta(C–H)_{ip}$; 532, (s), $\delta(C–H)_{oop}$. MS FAB$^+$ (NBA) {*m*/*z* [species]}: 413 $[2M + H]^+$, 207 $[M + H]^+$.

Synthesis of 5-(2-pyridylmethylene)-2-thioxothiazolidin-4-one IV

Pyridine-2-carbaldehyde (1.00 g, 9.34 mmol, 1 eq.) was added dropwise to a 100 cm^3 round bottomed flask containing rhodanine (1.24 g, 9.34 mmol, 1 eq.), glycine (0.70 g, 1 eq.), and sodium carbonate (0.49 g, 0.5 eq.). Effervescence was observed which became vigorous upon addition of distilled water (6 cm^3) yielding a solidified yellow mixture. The product was pulverised and after an addition of distilled water (4 cm^3), the suspension was stirred at reflux for 2 h. The product was allowed to cool to room temperature and the resulting precipitate was collected and washed with water, ethanol and diethyl ether and dried *in vacuo* to give a dull yellow powder which did not require further purification. Yield: 1.91 g, 92%, mp 257–260 °C (dec.). Found: C, 48.4; H, 2.7; N, 12.4%. Calc. for $C_9H_6N_2OS_2$: C, 48.6; H, 2.7; N, 12.6%. ^{1}H NMR (d_6-DMSO): δ 7.45 (H[11], ddd, $^3J(^1H,^1H)$ 8.2, $^4J(^1H,^1H)$ 4.5, $^5J(^1H,^1H)$ 1.0 Hz, 1H), 7.70 (H[6], s, 1H), 7.94 (H[12], d, $^3J(^1H,^1H)$ 7.9 Hz, 1H), 7.97 (H[10], dt, $^3J(^1H,^1H)$ 7.6, $^4J(^1H,^1H)$ 1.0 Hz, 1H), 8.80 (H[9], d, $^3J(^1H,^1H)$ 4.6 Hz, 1H), 13.70 (H[3] s(br), 1H). ^{13}C{^{1}H} NMR (d_6-DMSO): δ 202.66 (C2), 170.05 (C4), 151.75 (C7), 150.19 (C9), 138.26 (C11), 130.41 (C5), 128.83 (C12), 128.12 (C10), 124.66 (C6). ^{13}C solid state: δ 203.2 (C2), 168.8 (C4), 150.0 (C7, C9), 135.7 (C11),

Table 6 Crystal data, data collection and refinement parameters[a]

Data	I[b]	II[c]	III[c]	IV[c]	V[c]
Formula	$C_9H_7N_3O_2$	$C_9H_7N_3OS$	$C_9H_6N_2O_2S$	$C_9H_6N_2OS_2$	$C_9H_7N_3OS$
Formula weight	189.2	205.2	206.2	222.3	205.2
Crystal system	Monoclinic	Monoclinic	Triclinic	Triclinic	Triclinic
Space group	$P2_1/n$	$P2_1/n$	$P\bar{1}$	$P\bar{1}$	$P\bar{1}$
Cell dimensions					
a/Å	3.808(2)	4.709(3)	4.956(1)	3.882(1)	6.677(1)
b/Å	14.036(4)	10.278(4)	8.996(2)	11.038(1)	8.191(2)
c/Å	15.963(4)	18.676(11)	10.773(2)	11.425(1)	9.319(2)
α/deg	—	—	108.60(1)	76.45(1)	71.48(2)
β/deg	92.90(2)	92.11(5)	95.34(1)	87.34(1)	79.50(2)
γ/deg	—	—	95.93(1)	82.70(1)	73.31(2)
V/Å^3	852.1(3)	903.3(8)	448.7(1)	472.0(1)	460.6(2)
Z	4	4	2	2	2
Radiation used	Cu-Kα[d]	Cu-Kα[d]	Mo-Kα	Cu-Kα[d]	Cu-Kα
μ/mm^{-1}	0.91	2.93	0.33	4.83	2.87
No. of unique reflections					
Measured	1368	1417	2571	1391	1493
Observed, $\|F_o\| > 4\sigma(\|F_o\|)$	1093	1380	2200	1320	1406
R_1[e]	0.035	0.036	0.038	0.042	0.035
wR_2[f]	0.040[g]	0.097	0.106	0.117	0.094

[a] Details in common: graphite monochromated radiation, ω-scans, Siemens P4 diffractometer, 293 K. [b] Refinement based on F. [c] Refinement based on F^2. [d] Rotating anode source. [e] $R_1 = \Sigma||F_o| - |F_c||/\Sigma|F_o|$. [f] $wR_2 = \sqrt{\{\Sigma[w(F_o^2 - F_c^2)^2]/\Sigma[w(F_o^2)^2]\}}$; $w^{-1} = \sigma^2(F_o^2) + (aP)^2 + bP$. [g] The value given is for R_w; $w^{-1} = \sigma^2(F) + gF^2$.

133.5 (C5), 128.9 (C12), 125.9 (C10), 123.6 (C6). $^{15}N\{^1H\}$ MAS-CP NMR solid state: δ −70 (N8), −192 (N3). IR (ν_{max}/cm^{-1}): 3096, 3047, (m, br), ν(N–H); 1725, (s), ν(C=O); 1605, (s), ν(C=C); 1580, 1472, (s), ν(N=C, py); 1445, (s), δ(N–H); 1148, 1082, (s), ν(C=S); 1187, (s), ν(C–N–C); 917, (s), $\nu(C–S)_{ring}$; 878, 684, (s), δ(C=S); 781, (s), $\delta(C–H)_{ip}$; 523, (s), $\delta(C–H)_{oop}$. MS FAB$^+$ (NBA) {*m*/*z* [species]}: 223 $[M + H]^+$.

Synthesis of 2-amino-5-(2-pyridylmethylene)-4,5-dihydrothiazol-4-one V

Pyridine-2-carbaldehyde (9.22 g, 85.93 mmol, 1 eq.) was added dropwise to a flask containing pseudothiohydantoin (10.00 g, 96.03 mmol, 1.1 eq.), glycine (6.46 g, 1 eq.), and sodium carbonate (4.55 g, 0.5 eq.) followed by distilled water (10 cm^3). Upon stirring, vigorous effervescing was observed and the mixture stirred at room temperature for 1 h. The yellow–orange precipitate was collected and washed with water, ethanol, diethyl ether and dried *in vacuo* to give an off-white powder which did not require further purification. Yield: 16.33 g, 90%, mp 260–263 °C (dec.). Found: C, 52.7; H, 3.4; N, 20.3%. Calc. for $C_9H_7N_3OS$: C, 52.7; H, 3.4; N, 20.5%. ^1H NMR (d_6-DMSO): δ 7.34 (H[11], ddd, $^3J(^1H,^1H)$ 7.5, $^4J(^1H,^1H)$ 4.8, $^5J(^1H,^1H)$ 1.2 Hz, 1H), 7.63 (H[6], s, 1H), 7.74 (H[12], d, $^3J(^1H,^1H)$ 7.8 Hz, 1H), 7.86 (H[10], dt, $^3J(^1H,^1H)$ 7.7, $^4J(^1H,^1H)$ 1.8 Hz, 1H), 8.69 (H[9], d, $^3J(^1H,^1H)$ 4.6, 1H), 9.09 (NH, s, 1H), 9.32 (NH, s, 1H). $^{13}C\{^1H\}$ NMR (d_6-DMSO): δ 180.53 (C4), 180.01 (C2), 151.94 (C7), 149.21 (C9), 137.35 (C11), 133.38 (C5), 126.99 (C12), 125.83 (C6), 123.28 (C10). ^{13}C solid state: δ 183.6 (C4), 180.8 (C2), 152.9 (C7), 149.7 (C9), 136.2 (C11), 132.1 (C5), 129.45 (C12), 127.9 (C6), 124.5 (C10). $^{15}N\{^1H\}$ MAS-CP NMR solid state: δ −68 (N8), −160 (N3), −266 (N2). IR (ν_{max}/cm^{-1}): 3196, 2967, 2828, (br), ν(N–H); 2408, 2198, (m), ν(N–D); 1670, (s), ν(C=O); 1617, (s), ν(C=C); 1582, 1471, (s), ν(N=C, py); 1495, 1375, (s), δ(N–H); 1355, 1342, (s), δ(N–D); 1146, (s), ν(C–N–C); 895, (s), $\nu(C–S)_{ring}$; 780, (s), $\delta(C–H)_{ip}$ 553, 551, (s), $\delta(C–H)_{oop}$. MS FAB$^+$ (NBA) {*m*/*z* [species]}: 206 $[M+ H]^+$.

Synthesis of 5-(2-pyridylmethylene)-4-amino-2-imino-2,5-dihydrothiazole VI

Pyridine-2-carbaldehyde (1.00 g, 9.34 mmol, 1 eq.) was added dropwise to a flask containing 2-imino-4-amino-2,5-dihydrothiazole (1.42 g, 9.37 mmol, 1.1 eq.), glycine (1.40 g, 1 eq.), and sodium carbonate (1.00 g, 0.5 eq.) followed by distilled water (5 cm^3). Upon stirring, the resulting orange mixture started to change colour to red. At this point, a further 20 cm^3 of distilled water was added and the mixture stirred at room temperature for a further 10 minutes. The resulting orange precipitate was collected and washed with water, ethanol, diethyl ether and dried *in vacuo* to give an orange powder which did not require further purification. Yield: 1.15 g, 61% (with respect to the aldehyde), mp 180 °C (dec.). Found: C, 44.7; H, 5.2; N, 23.4%. Calc. for $(C_9H_8N_4S)\cdot 2H_2O$: C, 45.0; H, 5.0; N, 23.3%. ^1H NMR (d_6-DMSO): δ 7.38 (H[11], ddd, $^3J(^1H,^1H)$ 6.0, $^4J(^1H,^1H)$ 2.0 Hz, 1H), 7.54 (H[12], d, $^3J(^1H,^1H)$ 7.9 Hz, 1H), 7.80 (H[6], s, 1H), 7.91 (H[10], dt, $^3J(^1H,^1H)$ 7.6, $^4J(^1H,^1H)$ 1.6 Hz, 1H), 8.75 (H[9], d, $^3J(^1H,^1H)$ 4.3, 1H); (d_7-DMF): δ 7.33 (H[11], ddd, $^3J(^1H,^1H)$ 5.0, $^4J(^1H,^1H)$ 1.0 Hz, 1H), 7.56 (H[12], d, $^3J(^1H,^1H)$ 7.9 Hz, 1H), 7.87 (H[10], dt, $^3J(^1H,^1H)$ 7.7, $^4J(^1H,^1H)$ 1.7 Hz, 1H), 8.00 (H[6], s, 1H), 8.75 (H[9], d, $^3J(^1H,^1H)$ 4.9, 1H); (d_4-acetic acid): δ 7.42 (H[11], ddd, $^3J(^1H,^1H)$ 5.0, $^4J(^1H,^1H)$ 2.0 Hz, 1H), 7.73 (H[12], d, $^3J(^1H,^1H)$ 7.9 Hz, 1H), 7.92 (H[10], dt, $^3J(^1H,^1H)$ 7.7, $^4J(^1H,^1H)$ 1.8 Hz, 1H), 8.28 (H[6], s, 1H), 8.75 (H[9], d, $^3J(^1H,^1H)$ 4.3, 1H). $^{13}C\{^1H\}$ NMR (d_6-DMSO): δ 175.88 (C2), 172.49 (C4), 152.89 (C7), 149.85 (C9), 137.92 (C11), 134.86 (C5), 127.14 (C12), 124.00 (C10), 122.63 (C6). ^{13}C solid state: δ 180.8 (C2), 172.5 (C4), 152.7 (C7), 149.1 (C9), 137.9 (C11), 131.6 (C5), 127.1 (C10,12), 120.0 (C6). $^{15}N\{^1H\}$ MAS-CP NMR solid state: δ −68 (N8), −156 (N3), −285 (N2,4). IR (ν_{max}/cm^{-1}): 3600–2600, (vs, br), ν(N–H, hydrogen bonded); 1604, (s), ν(C=C); 1583, 1469, (s), ν(N=C, py); 1511, 1434, 1351, (s), δ(N–H); 1151, (s), ν(C–N–C); 896, 867, (s), $\nu(C–S)_{ring}$; 777, (s), $\delta(C–H)_{ip}$ 528, (s), $\delta(C–H)_{oop}$; other non assigned bands are: 1286, 1066, (m, br); 1417, 1247, 1099, (m); 1020, 993, 740, 727, 690, 647, 617, 484, (w). Accurate MS FAB$^+$ (NBA) {*m*/*z* [species]}: 205.0558 $[M + H]^+$.

X-Ray crystallographic details

Table 6 provides a summary of the crystal data, data collection, and refinement parameters for compounds **I**–**V**, data in each case having been corrected for Lorentz and polarization factors, and for absorption as indicated. Details of the treatment of structures **I** [52] and **V** [58] have been given elsewhere and so will not be repeated here. Structures **II**, **III** and **IV** were solved by direct methods and their non-hydrogen atoms were refined anisotropically using full matrix least-squares based on F^2. The

positions of the N–H hydrogen atoms in all the structures were determined from ΔF maps and were refined isotropically subject to an N–H distance constraint. The positions of the remaining hydrogen atoms were idealised, assigned isotropic thermal parameters [$U(H) = 1.2U_{eq}(C)$] and allowed to ride on their parent carbon atoms. Computations were carried out using the SHELXTL PC program system.[90]

Acknowledgements

The EPSRC is thanked for financial support and BP plc for generously endowing DMPMs Chair. We thank University of London Intercollegiate Research Services for the provision of facilities for solid state NMR spectroscopy.

References

1 J. L. Atwood, J. E. D. Davies, D. D. MacNicol and F. Vögtle, *Comprehensive Supramolecular Chemistry*, ed. J.-M. Lehn, Pergamon, Oxford, 1996.
2 Y. L. Chang, M.-A. West, F. W. Fowler and J. W. Lauher, *J. Am. Chem. Soc.*, 1993, **115**, 5991.
3 M. Vaida, L. J. W. Shimon, J. Van Mil, K. Ernst-Barbera, L. Addadi, L. Leiserowitz and M. Lahav, *J. Am. Chem. Soc.*, 1989, **111**, 1029.
4 J. A. Zerkowski, C. T. Seto and G. M. Whitesides, *J. Am. Chem. Soc.*, 1990, **112**, 9025.
5 C. T. Seto and G. M. Whitesides, *J. Am. Chem. Soc.*, 1990, **112**, 6409.
6 F. Garcia-Tellado, S. J. Geib, S. Goswami and A. D. Hamilton, *J. Am. Chem. Soc.*, 1991, **113**, 9265.
7 J.-M. Lehn, M. Mascal, A. DeCian and J. Fischer, *J. Chem. Soc., Perkin Trans. 2*, 1992, 461.
8 J.-M. Lehn, M. Mascal, A. DeCian and J. Fischer, *J. Chem. Soc., Chem. Commun.*, 1990, 479.
9 C. Fouquey, J.-M. Lehn and A.-M. Levelut, *Adv. Mater.*, 1990, **2**, 25.
10 M. Simard, D. Su and J. D. Wuest, *J. Am. Chem. Soc.*, 1991, **113**, 4696.
11 J. A. Zerkowski, C. T. Seto, D. A. Wierda and G. M. Whitesides, *J. Am. Chem. Soc.*, 1991, **113**, 712.
12 Y. Ducharme and J. D. Wuest, *J. Org. Chem.*, 1988, **53**, 5789.
13 M. Gallant, M. T. P. Biet and J. D. Wuest, *J. Org. Chem.*, 1991, **56**, 2284.
14 J. A. Zerkowski, C. T. Seto and G. M. Whitesides, *J. Am. Chem. Soc.*, 1992, **114**, 5473.
15 G. M. Whitesides, J. P. Mathias and C. T. Seto, *Science*, 1991, **254**, 1312.
16 F. Persico and J. D. Wuest, *J. Org. Chem.*, 1993, **58**, 95.
17 M. Scoponi, E. Polo, F. Pradella, V. Bertolasi, V. Carassiti and P. Goberti, *J. Chem. Soc., Perkin Trans. 2*, 1992, 1127.
18 V. A. Russell, M. C. Etter and M. D. Ward, *J. Am. Chem. Soc.*, 1994, **116**, 1941.
19 A. S. Batsanov, N. Svenstrup, J. Lau, J. Becher, M. R. Bryce and J. A. K. Howard, *J. Chem. Soc., Chem. Commun.*, 1995, 1201.
20 C. T. Seto and G. M. Whitesides, *J. Am. Chem. Soc.*, 1993, **115**, 905.
21 C. T. Seto, J. P. Mathias and G. M. Whitesides, *J. Am. Chem. Soc.*, 1993, **115**, 1321.
22 S. K. Chang and A. D. Hamilton, *J. Am. Chem. Soc.*, 1988, **110**, 1318.
23 S. J. Geib, S. C. Hirst, C. Vicent and A. D. Hamilton, *J. Chem. Soc., Chem. Commun.*, 1991, 1283.
24 E. Fan, S. A. Van Arman, S. Kincaid and A. D. Hamilton, *J. Am. Chem. Soc.*, 1993, **115**, 369.
25 S. J. Geib, C. Vicent, E. Fan and A. D. Hamilton, *Angew. Chem., Int. Ed. Engl.*, 1993, **32**, 119.
26 C. B. Aakeröy and K. R. Seddon, *Chem. Soc. Rev.*, 1993, **22**, 397.
27 J. Bernstein, R. E. Davis, L. Shimoni and N.-L. Chang, *Angew. Chem., Int. Ed. Engl.*, 1995, **34**, 1555.
28 D. S. Lawrence, T. Jiang and M. Levett, *Chem. Rev.*, 1995, **95**, 2229.
29 J. C. MacDonald and G. M. Whitesides, *Chem. Rev.*, 1994, **94**, 2383.
30 M. C. Etter, *Acc. Chem. Res.*, 1990, **23**, 120.
31 E. Fan, C. Vicent, S. J. Geib and A. D. Hamilton, *Chem. Mater.*, 1994, **6**, 1113.
32 A. Houlton, D. M. P. Mingos, A. J. P. White and D. J. Williams, *Transition Met. Chem.*, 1994, **19**, 653.
33 A. Houlton, D. M. P. Mingos and D. J. Williams, *J. Chem. Soc., Chem. Commun.*, 1994, 503.
34 C.-W. Chan, D. M. P. Mingos, A. J. P. White and D. J. Williams, *J. Chem. Soc., Dalton Trans.*, 1995, 2469.
35 J. E. McGrady and D. M. P. Mingos, *J. Chem. Soc., Perkin Trans. 2*, 1996, 355.
36 A. D. Burrows, D. M. P. Mingos, A. J. P. White and D. J. Williams, *J. Chem. Soc., Dalton Trans.*, 1996, 149 and unpublished results.
37 C.-W. Chan, D. M. P. Mingos, A. J. P. White and D. J. Williams, *Polyhedron*, 1996, **15**, 1753.
38 A. D. Burrows, D. M. P. Mingos, A. J. P. White and D. J. Williams, *Chem. Commun.*, 1996, 97.
39 C.-W. Chan, D. M. P. Mingos, A. J. P. White and D. J. Williams, *Chem. Commun.*, 1996, 81.
40 A. D. Burrows, D. M. P. Mingos, A. J. P. White and D. J. Williams, *J. Chem. Soc., Dalton Trans.*, 1996, 3805.
41 U. Koert, M. M. Harding and J.-M. Lehn, *Nature*, 1990, **346**, 339.
42 P. G. Desmartin, A. F. Williams and G. Bernardinelli, *New J. Chem.*, 1995, **19**, 1109.
43 A zinc(II) complex has been reported to take part in 'multi-point' recognition by binding to nucleobases through a combination of hydrogen bonds, π–π interactions *and* metal ion coordination: M. Shionoya, T. Ikeda, E. Kimura and M. Shiro, *J. Am. Chem. Soc.*, 1994, **116**, 3848.
44 B. F. Abrahams, S. J. Egan, B. F. Hoskins and R. Robson, *Chem. Commun.*, 1996, 1099.
45 M. Mascal, *Contemp. Org. Synth.*, 1994, **1**, 31.
46 M. Mascal, J. Hansen, P. S. Fallon, A. J. Blake, B. R. Heywood, M. H. Moore and J. P. Turkenburg, *Chem. Eur. J.*, 1999, **5**, 381.
47 U. Rychlewska, *J. Mol. Struct.*, 1999, **474**, 235.
48 S. V. Kolotuchin, P. A. Tiessen, E. E. Fenlon, S. R. Wilson, C. J. Loweth and S. C. Zimmerman, *Chem. Eur. J.*, 1999, **5**, 2537.
49 M. Mazik, D. Blaser and R. Boese, *Tetrahedron*, 1999, **55**, 7835.
50 M. Mazik, D. Blaser and R. Boese, *Tetrahedron*, 1999, **55**, 12771.
51 A. D. Burrows, C.-W. Chan, M. M. Chowdhry, J. E. McGrady and D. M. P. Mingos *Chem. Soc. Rev.*, 1995, 24, 329.
52 M. M. Chowdhry, A. D. Burrows, D. M. P. Mingos, A. J. P. White and D. J. Williams, *J. Chem. Soc., Chem. Commun.*, 1995, 1521.
53 M. M. Chowdhry, D. M. P. Mingos, A. J. P. White and D. J. Williams, *Chem. Commun.*, 1996, 899.
54 S. Ulvenlund, A. S. Georgopoulou, D. M. P. Mingos, I. Baxter, S. E. Lawrence, A. J. P. White and D. J. Williams, *J. Chem. Soc., Dalton Trans.*, 1998, 1869.
55 J. E. McGrady and D. M. P. Mingos, *J. Chem. Soc., Perkin Trans. 2*, 1996, 355.
56 T. J. Murray and S. C. Zimmerman, *J. Am. Chem. Soc.*, 1992, **114**, 4010.
57 J. Pranata, S. G. Wierschke and W. L. Jorgenson, *J. Am. Chem. Soc.*, 1991, **113**, 2810.
58 Investigations have been carried out to determine the tautomeric identity of **V** both in solution and the solid state. See M. M. Chowdhry, D. M. P. Mingos, A. E. Aliev, A. J. P. White and D. J. Williams, *J. Chem. Soc., Perkin Trans. 2* (DOI: 10.1039/b004368k).
59 H. H. Merritt, T. J. Putnam and W. G. Bywater, *J. Pharmacol.*, 1945, **84**, 67.
60 T. J. Putnam and H. H. Merritt, *Science*, 1937, **85**, 525.
61 H. B. Lewis, *J. Biol. Chem.*, 1912, **13**, 347.
62 H. B. Lewis, *J. Biol. Chem.*, 1913, **14**, 245.
63 Société pour l'industrie chimique à Bâle, *Swiss Pat.* 296688, 1939.
64 Société pour l'industrie chimique à Bâle, *Br. Pat.* 330883, 1942.
65 W. D. Stewart, *US Pat.* 2430591, 1947.
66 E. I. du Pont de Nemours and J. F. Walker, *Br. Pat.* 564424, 1944.
67 H. V. Wood and W. O. Drake, *US Pat.* 3560470, 1971.
68 E. I. du Pond de Nemours and J. F. Walker, *French Pat.* 1410426, 1965.
69 F. C. Brown, *Chem. Rev.*, 1961, **61**, 463 and references therein.
70 H. Thielemann, *Sci. Pharm.*, 1971, **39**, 8.
71 M. T. Montaña González, J. L. Gómez Ariza, F. Pino and R. Garcia Villanova, *Talanta*, 1978, **25**, 331 and references therein.
72 S.-F. Tan, K.-P. Ang and G.-F. How, *J. Phys. Org. Chem.*, 1990, **3**, 559.
73 J. S. Casas, E. E. Castellano, A. Macías, N. Playá, A. Sánchez, J. Sordo, J. M. Varela and J. Zukerman-Schpector, *Inorg. Chim. Acta*, 1995, **238**, 129.
74 M. M. Chowdhry, PhD Thesis, Imperial College, University of London, 1997.
75 N. Valls, V. M. Segarra, E. Alcalde and A. Marin, *J. Prakt. Chem.*, 1985, **327**, 251.
76 K. T. Potts, S. A. Nye and K. A. Smith, *J. Org. Chem.*, 1992, **57**, 3895.
77 A. P. Cuthbertson, C. Glidewell and D. C. Liles, *Acta Crystallogr., Sect. B*, 1982, **38**, 2281.
78 A. P. Cuthbertson, C. Glidewell and D. C. Liles, *Acta Crystallogr., Sect. C*, 1983, **39**, 106.

79 L. Latos-Grazynski, J. Lizowski, L. Szterenberg, M. M. Olmstead and A. L. Balch, *J. Org. Chem.*, 1991, **56**, 4043.
80 Y. Yamashita, K. Ono, S. Tanaka, K. Imaeda, H. Inokuchi and M. Sano, *J. Chem. Soc.*, *Chem. Commun.*, 1993, 1803.
81 Y. Yamashita, S. Tanaka, K. Imaeda, H. Inokuchi and M. Sano, *J. Org. Chem.*, 1992, **57**, 5517.
82 Y. Yamashita, S. Tanaka, K. Imaeda, H. Inokuchi and M. Sano, *J. Chem. Soc.*, *Chem. Commun.*, 1991, 1132.
83 Y. Yamashita, K. Ono, S. Tanaka, K. Imaeda and H. Inokuchi, *Adv. Mat.*, 1994, **6**, 295.
84 Y. Yamashita and S. Tanaka, *Chem. Lett.*, 1993, 73.
85 K. Ono, S. Tanaka, K. Imaeda and Y. Yamashita, *J. Chem. Soc.*, *Chem. Commun.*, 1994, 899.
86 Y. Yamashita, S. Tanaka, K. Imaeda, H. Inokuchi and M. Sano, *Chem. Lett.*, 1992, 419.
87 V. Y. Popkova, P. M. Dolgushin, M. Y. Antipin, A. I. Yanovsky and Y. T. Struchkov, *Heterocycles*, 1995, **40**, 1015.
88 C. Avendaño, M.T. Ramos, J. Elguero, M. L. Jimeno, J. Bellanato and F. Florencio, *Can. J. Chem.*, 1988, **66**, 1467.
89 P. J. M. W. L. Birker, *Inorg. Chem.*, 1977, **16**, 2478.
90 SHELXTL PC version 5.03, Siemens Analytical X-Ray Instruments, Inc., Madison, WI, 1994.